Nanoscale

COMMUNICATION

View Article Online
View Journal

Cite this: DOI: 10.1039/d0nr00902d

Received 2nd February 2020,
Accepted 18th March 2020

DOI: 10.1039/d0nr00902d

rsc.li/nanoscale

Nanometer control in plasmonic systems through discrete layer-by-layer macrocycle–cation deposition†

Steven J. Barrow, ‡§[a] Aniello Palma,¶‡[a] Bart de Nijs,[b] Rohit Chikkaraddy,[b] Richard W. Bowman,‖[b] Jeremy J. Baumberg[b] and Oren A. Scherman *[a]

In this work, we demonstrate that coordination interactions between Fe^{3+} and cucurbit[7]uril (CB[7]) can be utilised to build up defined nanoscale spacing layers in metallic nanosystems. We begin by characterising the layer-by-layer deposition of CB[7] and $FeCl_3{\cdot}6H_2O$ coordination layers through the use of a Quartz-Crystal Microbalance (QCM) and contact angle measurements. We then apply this layered structure to accurately control the spacing, and thus optical properties, of gold nanoparticles in a Nanoparticle-on-Mirror (NPoM) structure, which is demonstrated *via* normalising plasmon resonance spectroscopy.

Controlling spacing in assembled nano-scale systems remains a fundamental scientific challenge. Obtaining reproducible spacings is of utmost importance as the optical properties of plasmonic nano-structures depend on the spacing between plasmonic resonators, and thus control of these properties is largely related to our ability to reliably control inter-particle spacing.[1–3] Near-field confinement of incident electromagnetic radiation in the gaps between plasmonic resonators, termed 'hot spots', become more intense with decreasing gap size, magnifying Raman signals *via* Surface Enhanced Raman Scattering (SERS).[4] Rigid macrocycles known as cucurbit[*n*]urils (CB[*n*]s) have proven to be dynamic self-assembly motifs for nanoparticle systems,[5–7] providing well defined spacings that can be difficult to achieve with other methods.

CB[*n*]s are a family of macrocyclic compounds consisting of *n* number of glycoluril units, bound together by 2*n* methylene bridges, that have a well-defined height of 0.91 nm.[5] Due to their ability to encapsulate various guest species,[8] CB[*n*]s have been used to create assemblies of nanoparticles based on complex formation,[7] as well as through direct aggregation *via* the CB[*n*] molecules themselves.[5,6,9] Given their rigid structure and fixed height, CB[*n*]s yield reliable interparticle spacings of approximately 1 nm, which is ideal for producing strong coupling in nanoparticle systems, and intense hot spots;[10,11] however, reliable spacings beyond 1 nm in an incremental manner have yet to be realised.

The dipolar nature of the carbonyl-fringed portals of CB[*n*]s make them highly attractive for cation binding through the ion–dipole interactions, a well-established area of research.[12] Indeed, the first reports of CB[*n*] binding involved metal cations acting as 'lids' bound to the portals of CB[*n*].[13] Alkali metals,[13,14] alkaline earth metals,[15–17] transition metals,[17–19] lanthanides and actinides,[17,20–22] as well as ammonium and imidazolium ions[23] have been shown to bind to CB[*n*] portals, and are often required to enhance the solubility of the poorly water soluble CB[*n*]s. Despite intense research, few metal cations have been found that can bind to the portals of CB[7]. Coordination complexes with CB[7] require the use of exotic cations (lanthanides, uranium dioxide, *etc.*) in addition to $CdCl_4^{-2}$ and other dianions as stabilizer species in multi-step syntheses.

Given the ability of CB[*n*]s to bind to metal cations in the formation of 1 dimensional coordination compounds, and their well defined height, we demonstrate here that CB[7] can be used to create well-defined nanoparticle spacings with stepwise nanometer control *via* macrocycle–cation coordination. Furthermore, we show that this can be done in a simple manner using $FeCl_3{\cdot}6H_2O$ with no stabilizer dianions required. The interaction of CB[7] and Fe^{3+} represents a novel coordination compound, and thus we begin by characterising its structure. We then demonstrate that CB[7] and Fe^{3+} can be

[a]*Melville Laboratory for Polymer Synthesis, Department of Chemistry, University of Cambridge, CB2 1EW, UK. E-mail: oas23@cam.ac.uk*
[b]*Nanophotonics Centre, Cavendish Laboratory, University of Cambridge, CB3 0HE, UK*

†Electronic supplementary information (ESI) available. See DOI: 10.1039/D0NR00902D

‡Authors contributed equally.

§Current address: School of Applied Chemistry and Environmental Science, RMIT University, Melbourne, 3000, Australia
¶Current address: School of Physical Sciences, Ingram Building, University of Kent, Canterbury, Kent, CT2 7NH, UK
‖Current address: Department of Physics, University of Bath, BA2 7AY, UK

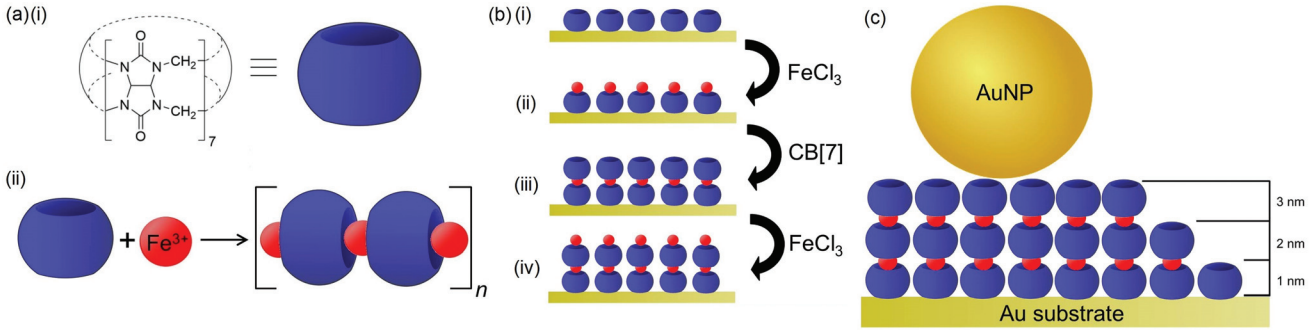

Fig. 1 (a) (i) The chemical structure of CB[7] is shown. (ii) A coordination complex forms when Fe^{3+} and CB[7] are mixed in water. (b) Schematic of the layer-by-layer process used to build up coordination complexes of CB[7] and $FeCl_3{\cdot}6H_2O$ onto gold substrates. (c) An illustration highlighting that surface deposited CB[7]–Fe^{3+} can be used to yield well defined spacings with nanometer control in plasmonic systems consisting of a gold film and a gold nanoparticle.

sequentially deposited onto a gold substrate in a layer-by-layer fashion through a Quartz Crystal Microbalance (QCM) study in conjunction with contact angle measurements. Finally, we use Normalising Plasmon Resonance Spectroscopy to probe not only the spacing in plasmonic structures on the nanoscale, but also demonstrate the changing refractive index of this system as the number of deposited layers increases.

The chemical structure of CB[7] is shown in Fig. 1(a)(i). The carbonyl groups present at the portals of the macrocycle favour ion–dipole binding with cations, which can lead to the formation of 1 dimensional coordination complexes, highlighted in Fig. 1(a)(ii). We have developed a method whereby such coordination complexes can be deposited in a step-wise manner onto a gold substrate. Firstly, a gold substrate is immersed in a 1 mM CB[7] aqueous solution Fig. 1(b)(i), rinsed, then placed in a 1 mM aqueous solution of $FeCl_3{\cdot}6H_2O$. The substrate is again rinsed and the deposition steps repeated to create the coordination complex, with a height that is dependant on the number of CB[7] molecules within the deposited spacing layer (a detailed experimental method is given in the ESI†). Noting that CB[7] has a rigid molecular structure with a well defined height of 0.91 nm, the CB[7]–Fe^{3+} complex can then be utilised in obtaining rigid molecular spacings in Nanoparticle on Mirror (NPoM) plasmonic systems, consisting of a metal nanoparticle on a metal film, where reliable spacings in between the two plasmonic elements is crucial in controlling the optical properties of the system. This forms an ideal 'plasmonic ruler' to quantify the spacer height.

Crystals were grown from a solution of water DMF and analysed using single-crystal X-ray diffraction. Initial experiments using laboratory equipment (microfocus source, CuKα radiation) indicated primitive lattice parameters $a \approx b \approx c \approx 70.4$ Å^3, $\alpha \approx \beta \approx \gamma \approx 109.5°$, volume $\approx 272\,000$ Å^3. This corresponds to an apparent I-centred cubic unit cell with $a = b = c \approx 81.4$ Å. On the laboratory equipment, diffraction was observed to approx. 1.5 Å, which was insufficient to make any progress with structure solution. A crystal was therefore analysed at Diamond Light Source (Beamline I19). This indicated the same lattice parameters, with diffraction data observed to approx. 1.0 Å. Systematic absence conditions suggest the space group to be $Ia\bar{3}d$. The very large unit-cell volume indicates a large number of formula units within the unit cell. Even for space group $Ia\bar{3}d$, with multiplicity 96 for a general equivalent position, there must be several formula units in the asymmetric unit. Inclusion of solvent molecules in the crystal is of course likely, and clearly the structure is complex. Despite all efforts, we have not to date been able to obtain any structure from the synchrotron data. It is possible that the crystals could be subject to twinning, but the apparent quality of the fit for the lattice parameters and the consistency of the result for several data sets under different analysis conditions may also indicate that the determined lattice parameters are correct. Certainly the lattice appears to be different from any known structure for CB[7] (lattice parameters $a \approx 12.9$ Å, $b \approx 20.1$ Å, $c \approx 31.7$ Å, $\beta \approx 92.6°$), or $FeCl_3{\cdot}6H_2O$ (lattice parameters $a \approx 11.89$ Å, $b \approx 7.05$ Å, $c \approx 5.99$ Å, $\beta \approx 100.5°$),[24,25] suggesting the formation of a complex between CB[7] and $FeCl_3{\cdot}6H_2O$. The synchrotron diffraction data are made available *via* the Cambridge Data Depository (10.17863/CAM.24844).

QCM data, in conjunction with contact angle measurements, have been used to confirm that CB[7] and Fe^{3+} can be deposited in an alternating fashion onto a gold substrate to build up a discrete functionalised surface film with specific control over film thickness on a macroscopic scale. Fig. 2 shows changes in the frequency of a gold-plated quartz crystal after sequential exposure to separate solutions of CB[7] and $FeCl_3{\cdot}6H_2O$. Once a 1 mM solution of CB[7] is passed over the gold-plated quartz crystal, the frequency is seen to decrease and plateau. This behaviour is indicative of deposition of material onto the QCM and is attributed to the binding of CB[7], through its carbonyl-fringed portals, onto the gold surface. The affinity between CB[*n*]s and gold surfaces[26] is a well established phenomenon that has been researched intensely for the purposes of gold nanoparticle aggregation.[9,27,28] Once the frequency had plateaued, demonstrating maximum deposition of the initial CB[7] layer, a 1 mM solution of $FeCl_3{\cdot}6H_2O$ was introduced to the quartz crystal. Once again, a

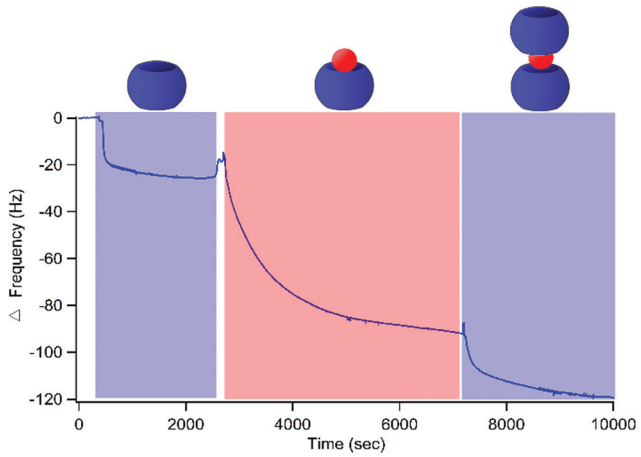

Fig. 2 Quartz crystal microbalance data demonstrating the layer-by-layer build up of CB[7]–Fe^{3+} nano-layers.

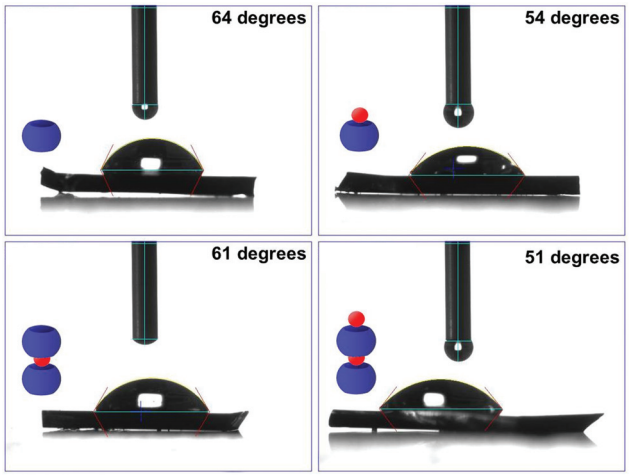

Fig. 3 Contact angle measurements highlighting the changes in hydrophobicity of a gold substrate after the layer-by-layer deposition of the CB–Fe^{3+} nanostructure.

consistent decrease in the frequency is evident, again suggesting the binding of material to the crystal. This further frequency decrease is a result of Fe^{3+} ions binding to the portals of the CB[7] molecules. This process can be repeated again by introducing a 1 mM CB[7] solution, which can bind through to the deposited Fe^{3+} layer, resulting in another decrease in the frequency of the quartz crystal. These results indicate that CB[7] and Fe^{3+} solutions can be deposited sequentially onto a gold film using a layer-by-layer methodology. Moreover, given that the cavities of the CB[*n*] macrocycles remain empty when forming coordination polymers, preformed CB[7] inclusion complex with a guest species in its cavity can be used to form these layer-by-layer coordination spacing layers. QCM data shown in the ESI† highlights that layered CB[7]–Fe_3^{+} structures also form when the CB[7] has ferrocene encapsulated within.

Contact angle measurements presented in Fig. 3 highlight the changes in hydrophobicity of a gold substrate after the deposition of the CB[7]–Fe^{3+} layered structure. Fig. 3(a) shows that the contact angle of a CB[7]-coated substrate is 64°, which decreases to 54° (Fig. 3(b)) when Fe^{3+} cations are deposited on top. The contact angle can then be switched back to 61° by the introduction of another CB[7] layer (Fig. 3(c)), and then decreased again to 51° through further Fe^{3+} deposition (Fig. 3(d)). Therefore, the contact angle can be switched between approximately 50 and 60° depending on whether CB[7] or Fe^{3+} is the terminating layer, which further supports the formation of 1 dimensional coordination polymers of CB[7] and Fe^{3+} on the gold substrate.

Both QCM and contact angle measurements support the layer-by-layer formation of CB[7]–Fe^{3+} structures on bulk gold surfaces, however it is pertinent to probe the integrity of the structure on the nano-scale. Therefore, Normalising Plasmon Resonance Spectroscopy, which has recently been employed to resolve the thickness and refractive index of layers of CB[7] in the NPoM geometry,[29] was utilised to demonstrate the applicability of the CB[7]–Fe^{3+} layers to nano-scale systems. The results of this can be seen in Fig. 4.

By collecting dark-field scattering spectra from individual nanoparticles in NPoM geometries and comparing the position and intensity of the coupled mode to finite difference time domain (FDTD) simulations the refractive index and gap spacing can be inferred. By collecting >1000 spectra per sample enough data can be analysed to identify differences between the samples and eliminate contributions from varying shape and size of individual nanoparticles. The peak at 533 nm is used as a reference point for normalisation since the transverse mode in this plasmonic system is less affected by the distance and refractive index of the gap. As can be seen in Fig. 4, the NPoM geometry consisting of a single layer of CB[7] (orange) yields coupled plasmon modes at 720–730 nm with an intensity ratio of 4.5. Based on FDTD simulations this would suggest a gap distance between 0.5–1 nm, which agrees well with the 0.91 nm height of CB[*n*] macrocycles. Upon addition of Fe^{3+} and a second layer of CB[7] (red) the peak decreases in intensity ratio to 3.8 with peak positions between 720–740 nm, matching an increase in refractive index of 0.3 and a distance increase of 1 nm, and a total gap distance of 2 nm. Adding another layer (pink) sees a further shift to an intensity ratio of 3 at 730–740 nm, correlating again to a change of 1 nm, and a total gap distance of 3 nm. Finally, having four CB[7] layers (blue) shifts the peak positions to 750 nm with intensity ratios just above 2. These results are in close agreement with the expected increase in gap distance, to a total of 4 nm, as layers of CB[7]·Fe^{3+} are stacked.

In summary, we have demonstrated that ion–dipole binding between CB[7] and Fe^{3+} cations can be utilised to create structures with discrete thickness on the nanoscale, which can be built up in a layer-by-layer fashion. We have shown that CB[7] and Fe^{3+} can be sequentially deposited onto a gold substrate, layer-by-layer, *via* a QCM study, in conjunction with contact

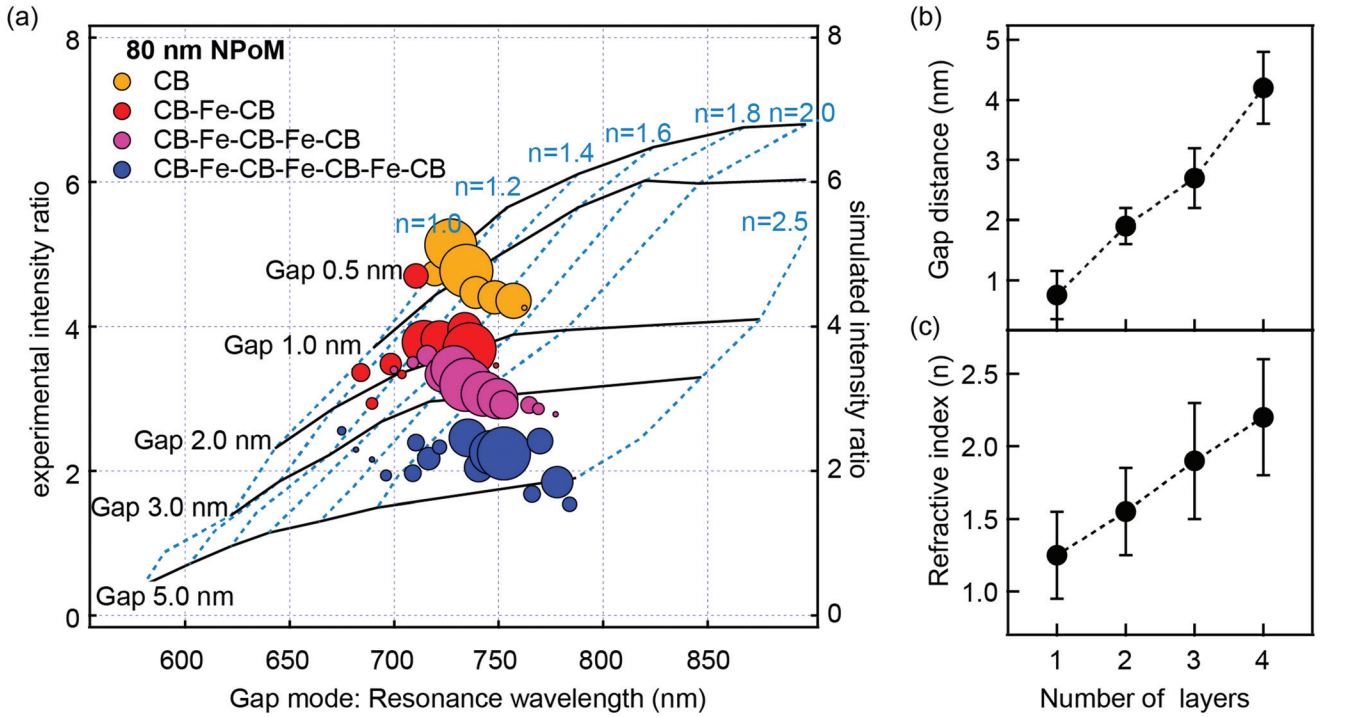

Fig. 4 Optical characterization of CB[7]-Fe^{3+} plasmonic nanogaps. (a) Intensity ratios between coupled and transverse modes in NPoM geometries for CB[7], CB[7]·Fe^{3+}·CB[7], CB[7]·Fe^{3+}·CB[7]·Fe^{3+}·CB[7] and CB[7]·Fe^{3+}·CB[7]·Fe^{3+}·CB[7]·Fe^{3+}·CB[7] spacers plotted against the resonance wavelength with results obtained from Finite Difference Time domain (FDTD) simulations using different spacer thickness and refractive indices. (b) Gap distance and (c) refractive index plotted *versus* number of CB[7] layers.

angle measurements. Finally, Normalising Plasmon Resonance Spectroscopy was used to demonstrate the build up of these structures on the nanoscale, highlighting the nanometer precision that can be obtained. This work highlights that control over spacings in nanostructures with nanometer precision can be realised through macrocycle–cation coordination. The next goal in this area will be to achieve the same level of spacing control in suspensions of nanoparticles.

Conflicts of interest

There are no conflicts to declare.

Acknowledgements

S. J. B. acknowledges support from the European Commission for a Marie Curie Fellowship (NANOSPHERE, 658360). A. P. and O. A. S. acknowledge an ERC starting investigator grant (ASPiRe 240629) and EPSRC Programme Grant (NOtCH, EP/L027151/1) for support. RC acknowledges support from the Dr Manmohan Singh scholarship from St. John's College. BdN acknowledges support from the Leverhulme Trust and the Isaac Newton trust ECF. The authors would like to thank Dr Helena Shephered for valuable discussions.

References

1 W. Rechberger, A. Hohenau, A. Leitner, J. R. Krenn, B. Lamprecht and F. R. Aussenegg, *Opt. Commun.*, 2003, **220**, 137–141.
2 J. J. Baumberg, J. Aizpurua, M. H. Mikkelsen and D. R. Smith, *Nat. Mater.*, 2019, **18**, 668–678.
3 C. Readman, B. de Nijs, I. Szabo, A. Demetriadou, R. Greenhalgh, C. Durkan, E. Rosta, O. Scherman and J. Baumberg, *Nano Lett.*, 2019, **19**, 2051–2058.
4 S. Kasera, F. Biedermann, J. J. Baumberg, O. A. Scherman and S. Mahajan, *Nano Lett.*, 2012, **12**, 5924–5928.
5 R. W. Taylor, T. C. Lee, O. A. Scherman, R. Esteban, J. Aizpurua, F. M. Huang, J. J. Baumberg and S. Mahajan, *ACS Nano*, 2011, **5**, 3878–3887.
6 S. T. Jones, R. W. Taylor, R. Esteban, E. K. Abo-Hamed, P. H. H. Bomans, N. A. J. M. Sommerdijk, J. Aizpurua, J. J. Baumberg and O. A. Scherman, *Small*, 2014, **10**, 4298–4303.
7 S. T. Jones, J. M. Zayed and O. A. Scherman, *Nanoscale*, 2013, **5**, 5299–5302.
8 S. J. Barrow, S. Kasera, M. J. Rowland, J. del Barrio and O. A. Scherman, *Chem. Rev.*, 2015, **115**, 12320–12406.
9 T. C. Lee and O. A. Scherman, *Chem. Commun.*, 2010, **46**, 2438–2440.
10 D. O. Sigle, S. Kasera, L. O. Herrmann, A. Palma, B. de Nijs, F. Benz, S. Mahajan, J. J. Baumberg and O. A. Scherman, *J. Phys. Chem. Lett.*, 2016, **7**, 704–710.

11 B. de Nijs, C. Carnegie, I. Szabo, D.-B. Grys, R. Chikkaraddy, M. Kamp, S. J. Barrow, C. A. Readman, M.-E. Kleemann, O. A. Scherman, E. Rost and J. J. Baumberg, *ACS Sens.*, 2019, **4**, 2988–2996.
12 X.-L. Ni, X. Xiao, H. Cong, L.-L. Liang, K. Cheng, X.-J. Cheng, N.-N. Ji, Q.-J. Zhu, S.-F. Xue and Z. Tao, *Chem. Soc. Rev.*, 2013, **42**, 9480–9508.
13 Y. M. Jeon, J. Kim, D. Whang and K. Kim, *J. Am. Chem. Soc.*, 1996, **118**, 9790–9791.
14 D. Whang, J. Heo, J. H. Park and K. Kim, *Angew. Chem., Int. Ed.*, 1998, **37**, 78–80.
15 O. A. Gerasko, A. V. Virovets, D. G. Samsonenko, A. A. Tripolskaya, V. P. Fedin and D. Fenske, *Russ. Chem. Bull.*, 2003, **52**, 585–593.
16 O. Danylyuk and V. P. Fedin, *Cryst. Growth Des.*, 2012, **12**, 550–555.
17 J. X. Liu, L.-S. Long, R.-B. Huang and L.-S. Zheng, *Cryst. Growth Des.*, 2006, **6**, 2611–2614.
18 H. J. Buschmann, E. Cleve, K. Jansen and E. Schollmeyer, *Anal. Chim. Acta*, 2001, **437**, 157–163.
19 O. A. Gerasko, E. A. Mainicheva, M. I. Naumova, M. Neumaier, M. M. Kappes, S. Lebedkin, D. Fenske and V. P. Fedin, *Inorg. Chem.*, 2008, **47**, 8869–8880.
20 P. Thuéry, *Cryst. Growth Des.*, 2009, **9**, 1208–1215.
21 Y. Liu, C.-J. Li, D.-S. Guo, Z.-H. Pan and Z. Li, *Supramol. Chem.*, 2007, **19**, 517–523.
22 D. G. Samsonenko, J. Lipkowski, O. A. Gerasko, A. V. Virovets, M. N. Sokolov, V. P. Fedin, J. G. Platas, R. Hernandez-Molina and A. Mederos, *Eur. J. Inorg. Chem.*, 2002, **2002**, 2380–2388.
23 K. Jansen, H. J. Buschmann, A. Wego, D. Döpp, C. Mayer, H. J. Drexler, H. J. Holdt and E. Schollmeyer, *J. Inclusion Phenom. Macrocyclic Chem.*, 2001, **39**, 357–363.
24 J. Kim, I. Jung, S. Kim, E. Lee, J. Kang, S. Sakamoto, K. Yamaguchi and K. Kim, *J. Am. Chem. Soc.*, 2000, **122**, 540–541.
25 M. D. Lind, *J. Chem. Phys.*, 1967, **47**, 990–993.
26 Q. An, G. Li, C. Tao, Y. Li, Y. Wu and W. Zhang, *Chem. Commun.*, 2008, 1989–1991.
27 V. Montes-García, J. Pérez-Juste, I. Pastoriza-Santos and L. M. Liz-Marzán, *Chem. – Eur. J.*, 2014, **20**, 10874–10883.
28 T. C. Lee and O. A. Scherman, *Chem. – Eur. J.*, 2012, **18**, 1628–1633.
29 B. de Nijs, R. W. Bowman, L. O. Herrmann, F. Benz, S. J. Barrow, J. Mertens, D. O. Sigle, R. Chikkaraddy, A. Eiden, A. Ferrari, O. A. Scherman and J. J. Baumberg, *Faraday Discuss.*, 2015, **178**, 185–193.